THE JOURNAL OF PHYSICAL CHEMISTRY B

Article

pubs.acs.org/JPCB

Role of Local Response in Ion Solvation: Born Theory and Beyond

Richard C. Remsing*,†,‡ and John D. Weeks*,‡,§

†Institute for Computational Molecular Science and Center for the Computational Design of Functional Layered Materials, Temple University, Philadelphia, Pennsylvania 19122, United States

‡Institute for Physical Science and Technology, University of Maryland, College Park, Maryland 20742, United States

§Department of Chemistry and Biochemistry, University of Maryland, College Park, Maryland 20742, United States

Supporting Information

ABSTRACT: The nature of ion solvation has drawn the interest of scientists for over a century, yet a thorough theoretical understanding is still lacking. In this work, we focus on the microscopic origins underlying ionic charge asymmetric and nonlinear response contributions to ion solvation free energies. We first derive an exact expression for the charging component of the ionic free energy, the free energy change when the Coulomb interactions between a fixed ion and the solvent are gradually "turned on". We then introduce the concept of a Gaussian test charge distribution, a generalization of the classical electrostatic point test charge that can be used to probe dielectric response in atomically detailed models. This enables the study of a thermodynamic cycle that isolates a linear and charge-symmetric contribution to the free energy that is well-described by Born-model-like dielectric continuum theories. We give a simple physical derivation of the classic Born model that locally relates the induced charge density in a linear dielectric model to the applied ionic charge distribution. The nonlinear response and charge asymmetric contributions to the ion solvation free energy are then examined in the remaining steps of the cycle and compared to classic thermodynamic cycles for this process using computer simulations. The insights provided by this work will aid the development of quantitative theories for the solvation of charged solutes.

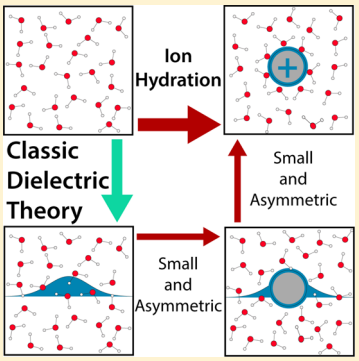

1. INTRODUCTION

Ions are at the heart of many biological and technological processes.[1−5] However, a complete understanding of the solvation of ionic solutes is lacking, despite being a subject of intense experimental and theoretical investigation for nearly a century. A major landmark in the theoretical description of ion solvation was the model developed by Born in 1920.[6] The Born model of ion solvation traditionally assumes the solvent is excluded from a spherical region around a point charge, corresponding to the excluded volume core of the ionic solute, while otherwise acting like a uniform linear dielectric in its response to the ionic charge. This macroscopic dielectric continuum theory (DCT) often yields estimates of solvation thermodynamic quantities in reasonable order of magnitude agreement with experiment, but is unable to describe many detailed features of ion solvation even qualitatively. The most notable example is the Born model's failure to capture the observed asymmetry of ion solvation free energies with respect to the sign of the ion charge that exists for multipolar solvents[7] (solvation in purely dipolar fluids is trivially symmetric), although extensions have been developed that treat this asymmetry with additional fitting parameters.[8,9]

Recent work has attempted to attribute a portion of the asymmetric nature of ion solvation to the surface potential of water arising from boundary interfaces far from the ion.[10−13] While this in principle can contribute to solvation thermodynamics, it has yet to be measured experimentally, and theoretical estimates of the surface potential have differed in both sign and magnitude.[14−21] Moreover, the local restructuring of water at the surface of even an uncharged ionic core generates a "broken symmetry" state[10,20−22] with a nonzero charge density that directly contributes to the charge asymmetry when the core is charged. These subtleties have led to intense theoretical investigations regarding the manner in which ion solvation free energies are estimated.[7,10,12,14,15,20−25] Despite these advances, our understanding of the microscopic origins and consequences of the asymmetries and nonlinearities associated with ion solvation thermodynamics remains incomplete.

In this paper, we first derive an exact expression for the charging component of the ionic free energy, the free energy change of a hypothetical process where the magnitude of the charge of a fixed ion in the solvent is gradually increased in going from an uncharged "ion core" to the fully charged ion. For the simple classical models considered here all the other non-electrostatic components of the ion−water interactions, including in particular van der Waals interactions as well as the harshly repulsive excluded volume interactions, remain unchanged during the charging process and characterize the "ion core" as the term is used in this paper. Both excluded volume and van der Waals

Special Issue: William M. Gelbart Festschrift

Received: March 3, 2016
Revised: May 15, 2016
Published: May 16, 2016

DOI: 10.1021/acs.jpcb.6b02238
J. Phys. Chem. B 2016, 120, 6238−6249

interactions are known to play important (and often competing) roles in the core contribution to the total ionic solvation free energy of realistic ions.[26]

Here we focus on the generally much larger charging contributions to the total solvation free energy where the charge asymmetries directly manifest themselves. For simplicity and to make most direct contact with the classical Born model, we consider simple hard-sphere-like models of the ion core, but inclusion of softer cores and van der Waals interactions would not qualitatively change any of our main conclusions. We examine here local contributions to the observed charge asymmetry and nonlinear effects and will consider the role of distant boundaries in a future publication.

We then give a new and simple physical derivation of the Born model that allows us to assess its strengths and weakness as a model for ion charging. We show in particular that Born-like models can be very accurate when considering the response to slowly varying Gaussian charge distributions rather than to δ-function point charges inside ion cores. We argue it may be both conceptually and practically useful to use Gaussian charges as the first step in a new thermodynamic cycle to determine a dominant and symmetric component for the total ion solvation free energy, to which nonlinearities and charge asymmetries make relatively small but very important corrections. These corrections are then isolated in the remaining steps of the cycle, allowing us to investigate their microscopic origins.

2. EXACT EXPRESSION FOR THE CHARGING COMPONENT OF IONIC FREE ENERGY

The electrostatic potential arising from a fixed ionic solute with a general uncharged core c and a charge distribution $\rho^Q(\mathbf{r})$ with total charge Q is

$$v^Q(\mathbf{r}) = \int d\mathbf{r}' \frac{\rho^Q(\mathbf{r}')}{|\mathbf{r} - \mathbf{r}'|} \tag{1}$$

Introducing a linear coupling parameter λ $(0 \le \lambda \le 1)$ multiplying the unit of ionic charge, the solute−solvent Coulomb interaction energy $\Psi_\lambda(\overline{\mathbf{R}})$ between a partially charged ion with potential $v_\lambda^Q(\mathbf{r}) \equiv \lambda v^Q(\mathbf{r})$ and the solvent with N_C full charges in a given configuration $\overline{\mathbf{R}}$ is given by

$$\Psi_\lambda(\overline{R}) = \int d\mathbf{r} v_\lambda^Q(\mathbf{r}) \rho^q(\mathbf{r}; \overline{\mathbf{R}}) \tag{2}$$

Here

$$\rho^q(\mathbf{r}; \overline{R}) = \sum_{i=1}^{N_C} q_i \delta(\mathbf{r} - \mathbf{r}_i(\overline{\mathbf{R}})) \tag{3}$$

is the configurational charge density. Note that $\Psi_\lambda(\overline{\mathbf{R}})$ is the only term in the solute−solvent Hamiltonian that depends explicitly on λ.

We now want to determine the free energy change $\Delta G^c(Q)$ on charging the core from the uncharged state $G^c_{\lambda=0}(Q) \equiv G^c_0$ to the fully charged state with $\lambda = 1$. Following standard coupling parameter methods we differentiate the exact partition function expression for the free energy $G^c_\lambda(Q)$ of the partially coupled system with respect to λ and immediately obtain

$$\frac{dG^c_\lambda}{d\lambda} = \left\langle \frac{d\Psi_\lambda(\overline{\mathbf{R}})}{d\lambda} \right\rangle_\lambda \tag{4}$$

$$= \int d\mathbf{r} v^Q(\mathbf{r}) \rho^q_\lambda(\mathbf{r}) \tag{5}$$

where $\langle\rangle_\lambda$ denotes a normalized ensemble average when the solute has coupling parameter (or charge state) λ and

$$\rho^q_\lambda(\mathbf{r}) \equiv \langle \rho^q(\mathbf{r}; \overline{\mathbf{R}}) \rangle_\lambda \tag{6}$$

is the ensemble-averaged solvent charge density. In eqs 4 and 5 we have noted that $v^Q_\lambda(\mathbf{r}) = \lambda v^Q(\mathbf{r})$ is linear in λ.

Integration of eq 5 over λ then yields an exact result that can be written as

$$\Delta G^c(Q) = \int d\mathbf{r} v^Q(\mathbf{r}) \rho^q_0(\mathbf{r}) + \int d\mathbf{r} v^Q(\mathbf{r}) \int_0^1 d\lambda \Delta\rho^q_\lambda(\mathbf{r})$$

$$\equiv \Delta G^c_P(Q) + \Delta G^c_I(Q) \tag{7}$$

Here $\Delta\rho^q_\lambda(\mathbf{r}) \equiv \rho^q_\lambda(\mathbf{r}) - \rho^q_0(\mathbf{r})$ is the change in the solvent charge density induced by charging the core from the uncharged $\lambda = 0$ state to the λ-state.

Since the charge density vanishes in a uniform bulk solvent, one can identify $\Delta G^c_P(Q)$ as the free energy that arises from interactions between the fully charged solute and the *pre-existing* solvent charge density $\rho^q_0(\mathbf{r})$ arising from boundaries that create structural and electrostatic inhomogeneities in the absence of solute charge.[21] These boundaries can be far from the solute, like the distant liquid−vapor interfaces or hard walls considered in several studies,[11,12] but the repulsive core of the uncharged solute (as well as van der Waals interactions if present) generates a particularly important local boundary that will induce a nonzero electrostatic response in a realistic solvent like water.[21] The $\Delta G^c_P(Q)$ term is typically linear in the solute charge Q, and is completely absent from the Born model and similar symmetric dielectric continuum treatments of solvent response.

The second term in eq 7 is the additional contribution to the charging free energy from local solvent perturbations $\Delta\rho^q_\lambda(\mathbf{r})$ *induced by changes in the solute charge*. This *induced* term $\Delta G^c_I(Q)$ would be expected to be symmetric and proportional to Q^2 for small enough Q. However, for charges typical of physical ions, additional asymmetric and nonlinear responses appear fundamentally due to solvent response to both electrostatic and nonelectrostatic interactions involving the ion and its core.[10,21,25,27,28] Thus, the form of the charging free energy in eq 7 allows us to separate the more symmetric and local charging-induced contributions to thermodynamic properties from the inherently asymmetric and often long-ranged contributions arising from interactions between the solute charge and pre-existing electrostatic boundaries. We focus on the former in this paper, initially as described by the Born model.

3. BORN MODEL FOR THE CHARGING FREE ENERGY

In our derivation of a Born-like model for the charging free energy $\Delta G^c(Q)$, we consider carrying out the same coupling parameter integration as in the previous section, where we now systematically charge a cavity of radius R in a dielectric from 0 to Q ($\lambda = 0$ to $\lambda = 1$). However, we additionally introduce some simplifying assumptions about the nature of the solvent and approximate the induced charge distribution. At $\lambda = 0$, the system consists of an infinite continuum dielectric solvent with an uncharged cavity at the origin. The Born model (incorrectly) assumes that because this cavity has no charge, it does not induce a dielectric response in the solvent. Thus, outside the cavity, the solvent charge density is taken to be uniform, with $\rho^q_0(\mathbf{r}) = 0$.

DOI: 10.1021/acs.jpcb.6b02238
J. Phys. Chem. B 2016, 120, 6238−6249

Now we consider the solvent response as the ion charge density is turned on. To arrive at the Born model we assume that the solvent responds linearly and locally to the solute charge density $\rho_\lambda^Q(\mathbf{r})$ at each overlapping position $\mathbf{r}$, in a manner dictated by the solvent dielectric constant ϵ. This means that the induced solvent charge density $\rho_\lambda^q(\mathbf{r})$ is simply

$$\rho_\lambda^q(\mathbf{r}) = -\left(1 - \frac{1}{\epsilon}\right)\rho_\lambda^Q(\mathbf{r}) \tag{8}$$

with the dielectric solvent locally screening or canceling all but a fraction $1/\epsilon$ of the applied charge distribution $\rho_\lambda^Q(\mathbf{r})$. In the next section we will derive and test this approximation directly for Gaussian charge distributions in SPC/E water and show that it can be very accurate for slowly varying Gaussians.

However, in the standard Born ion model, the ion charge $\rho_\lambda^Q(\mathbf{r})$ is usually assumed to be a δ-function point charge inside a cavity that excludes the dielectric so eq 8 cannot immediately be used. However, using Gauss' law, we can smear the charge of the ion uniformly over the surface of the cavity to obtain an equivalent solute charge distribution that now overlaps with the solvent at $r = R$ and has the same potential $v^Q(r) = Q/r$ for $r > R$

$$\rho_\lambda^Q(\mathbf{r}) = \begin{cases} \lambda Q \dfrac{\delta(r-R)}{4\pi r^2} & r \geq R \\ 0 & r < R \end{cases} \tag{9}$$

The usual Born expression for the charging free energy is obtained by simply inserting eqs 8 and 9 into eq 7, which gives

$$\Delta G^c(Q) = -Q^2\left(1 - \frac{1}{\epsilon}\right)\int_0^1 \mathrm{d}\lambda\lambda \int_R^\infty \frac{\delta(r-R)}{r} \tag{10}$$

$$= -\left(1 - \frac{1}{\epsilon}\right)\frac{Q^2}{2R} \tag{11}$$

In this interpretation the Born radius $R_B = R$ is a (charge-independent) measure of the region around the ion where solute−solvent interactions exclude most water molecules and need not necessarily coincide with determinations of ion core sizes in other contexts like crystal radii.

The above derivation clearly illustrates the major assumptions in the Born model, which manifest its deficiencies. One major assumption is that $\rho_0^q(\mathbf{r}) = 0$, which is known to be false. The electrostatic response to nonelectrostatic perturbations, like an uncharged ion core, have been heavily explored and are well-understood.[12,20,21] The other major assumption is the local linear response of the solvent to the applied ion charge distribution. This response is in fact nonlocal and nonlinear, as detailed further below. The invalidity of these assumptions is due to strong, short-ranged intermolecular interactions dominating the perturbations and subsequent response. Thus, in order for Born-like models to be valid, one needs to consider charge perturbations that vary slowly over molecular correlation lengths and can induce a linear response. We explore such distributions in the following section.

4. SOLVATION OF A GAUSSIAN TEST CHARGE

In contrast to harshly repulsive solute cores and strong, short-ranged electrostatic interactions from point charges, small continuous charge densities that vary slowly over molecular length scales need no shielding cores and are expected to induce a linear response in the solvent. One such slowly varying electrostatic interaction is that of a Gaussian charge distribution, with charge density $\rho_G^Q(r) \equiv Q\rho_G(r)$, where $\rho_G(r)$ is a Gaussian distribution with large width l

$$\rho_G(r) = \frac{1}{l^3\pi^{3/2}}e^{-r^2/l^2} \tag{12}$$

The potential from a Gaussian charge distribution, determined by eq 1, approaches that of a point charge of the same magnitude at distances greater than l and can be useful in determining thermodynamic properties of ion solvation, as discussed further in the next section.

Moreover, the potential from a Gaussian charge distribution does not have a singularity at its origin. Such a Gaussian charge distribution needs no shielding nonelectrostatic core and can be directly inserted even into an atomically detailed model of dielectric media with effective point charges on atomic sites, as in SPC/E water, in complete analogy to test charges considered in classical electrostatics texts.[29] A slowly varying distribution will not incur the large energy variations from insertions in the space outside or inside molecular cores that complicate analysis of experimental probes of the surface potential.[18] This same insertion cannot be carried out with a δ-function point charge unless its singularity is shielded by an ion core preventing overlap as in the Born model. Thus, we anticipate that insertion of a slowly varying Gaussian test charge distribution will generate a classic dielectric continuum-like response even in atomically detailed models.

As discussed in more detail below, these same qualitative features should apply to many other slowly varying charge distributions, but Gaussians have particularly simple properties that permit analytic calculations of the dielectric response. Gaussian charge distributions have long been used in many other contexts as well, including Ewald sum treatments of periodic boundary conditions for charged and polar systems,[30] in the development of polarizable versions of the simple point charge models of ions and water considered in this paper,[31−33] and even as coarse-grained descriptions of polyions.[34,35]

We now estimate the free energy change $\Delta G^l(Q)$ of inserting a Gaussian test charge with width l in a uniform solvent by linearly coupling its potential $v_G^Q(r)$ to a parameter λ, as done above. When $\lambda = 0$, the system is simply the bulk solvent only, and $\lambda = 1$ corresponds to a fully interacting Gaussian with charge Q in the solvent. The free energy in eq 7 can then be exactly written as

$$\Delta G^l(Q) = \int \mathrm{d}\mathbf{r} v_G^Q(r) \int_0^1 \mathrm{d}\lambda \rho_\lambda^q(\mathbf{r}) \tag{13}$$

where $\rho_\lambda^q(\mathbf{r})$ is the ensemble-averaged charge density at coupling parameter λ. Note that the $\rho_0^q(\mathbf{r})$ and $\Delta G_P(Q)$ terms appearing in eq 7 are rigorously zero here.

We can evaluate the free energy analytically by approximating the charge density induced by the electrostatic potential of the Gaussian test charge, $v_G^Q(r)$. Such an approximation is readily obtained by transforming to Fourier space and functionally expanding the charge density response to linear order in the solute potential

$$\hat{\rho}_\lambda^q(\mathbf{k}) \approx -\beta\hat{\chi}_0^{qq}(\mathbf{k})\hat{v}_G^{\lambda Q}(k) \tag{14}$$

where $\hat{f}(\mathbf{k})$ indicates the Fourier transform of $f(\mathbf{r})$. Here $\hat{v}_G^{\lambda Q}(k) = (4\pi\lambda Q/k^2)\mathrm{e}^{-(kl)^2/4}$, and $\hat{\chi}_0^{qq}(\mathbf{k})$ is the Fourier transform of the charge−charge linear response function

$$\chi_\lambda^{qq}(\mathbf{r}, \mathbf{r}') \equiv \langle \rho^q(\mathbf{r}; \bar{\mathbf{R}})\rho^q(\mathbf{r}'; \bar{\mathbf{R}})\rangle_\lambda \tag{15}$$

DOI: 10.1021/acs.jpcb.6b02238
J. Phys. Chem. B 2016, 120, 6238−6249

evaluated in the uniform bulk fluid ($\lambda = 0$). If the potential $v_G^Q(r)$ is slowly varying over typical nearest-neighbor distances, then the large k components of the charge density will contribute negligibly to the response. Under these conditions, the linear response function can be expanded to second order[36,37]

$$\hat{\chi}_0^{qq}(\mathbf{k}) \sim \hat{\chi}_0^{(0)qq} + k^2\hat{\chi}_0^{(2)qq} + O(k^4) \tag{16}$$

where $\hat{\chi}_0^{(0)qq} = 0$ due to neutrality, and $\hat{\chi}_0^{(2)qq} = -\frac{1}{6}\int d\mathbf{r} r^2 \chi_0^{qq}(r)$.

The second moment of the charge−charge linear response function is exactly related to the dielectric constant by a generalization of the Stillinger−Lovett moment conditions[37−41]

$$4\pi\beta\hat{\chi}_0^{(2)qq} = 1 - \frac{1}{\epsilon} \tag{17}$$

Thus, our final linear response theory approximation from eq 14 for the induced charge density is

$$\rho_\lambda^q(\mathbf{r}) \approx -\left(1 - \frac{1}{\epsilon}\right)\rho_G^{\lambda Q}(\mathbf{r}) \tag{18}$$

in agreement with the simple dielectric continuum screening arguments used above to derive the Born model. This illustrates how such a response to a slowly varying charge distribution can arise from microscopic principles.

We now evaluate the linear response theory prediction for $\Delta G^l(Q)$ for the Gaussian charge distribution by inserting eq 18 into eq 13 (and similarly for an arbitrary slowly varying charge distribution) and obtain

$$\Delta G^l(Q) = -\frac{Q^2}{l\sqrt{2\pi}}\left(1 - \frac{1}{\epsilon}\right) \tag{19}$$

for the solvation free energy of a Gaussian charge distribution. Other thermodynamic quantities of interest, like the solvation entropy, can readily be obtained in this level of approximation as illustrated in the Supporting Information.

Equation 19 can be used to define the width l_B of an equivalent Gaussian charge Born model with the same charging free energy as in eq 11, where

$$R_B = l_B\sqrt{\pi/2} \tag{20}$$

However, we anticipate that eq 19 for the inserted Gaussian energy will be much more accurate than the standard Born model prediction for an ion, because complications from the strong local forces associated with the ion core do not arise.

5. NUMERICAL VALIDATION OF THE GAUSSIAN TEST CHARGE MODEL

In this and later sections it is useful to use the "cup" notation of ref 42 to denote the solvation or field insertion free energy change of a system in a general external field $\phi(\mathbf{r})$ relative to the pure solvent. Thus, if $\phi(\mathbf{r})$ denotes the solute−solvent interaction field from a fixed solute, the solvation free energy $\breve{G}[\phi] \equiv G[\phi] - G[\phi = 0]$ gives the difference in free energy between the full solvent−solute system and the pure solvent in zero solute field. Introducing a simplified notation, the insertion free energy $\Delta G^l(Q)$ in eq 13 of the Gaussian charge field with width l is written here as $\breve{G}^l$. Similarly the free energy change of inserting an uncharged core c is denoted as $\breve{G}^c$. A core with an embedded point charge p is denoted as cp, and a core with a Gaussian is cl. We now numerically examine the structural and thermodynamic response of SPC/E water to the insertion of a Gaussian test charge of width l and magnitude Q.

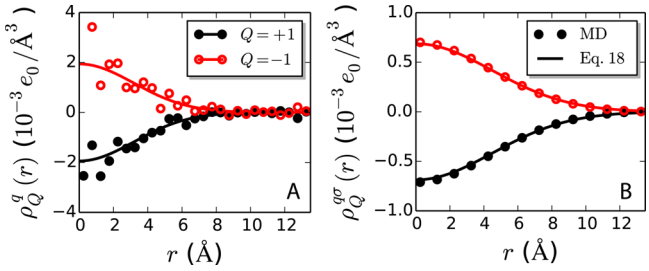

Figure 1. (A) Bare and (B) Gaussian smoothed charge densities in SPC/E water induced by a Gaussian test charge of magnitude $Q = \pm 1$ and width $l = 4.5$ Å. Data points are simulation results while lines are analytic approximations obtained through the use of eq 18. Smoothed charge densities were calculated using a smoothing length of $\sigma = l$.

The charge density response from eq 18 is compared with those from simulations of the SPC/E water model in Figure 1A. Despite the simulation noise at small r, the charge densities computed from simulations closely follow those predicted by eq 18, illustrating that the response to a Gaussian test charge closely follows DCT. This additionally justifies the concept of a Gaussian charge distribution being the analogue of a classical test charge for atomistic models.

The continuum nature of the solvent response is better illustrated by considering only its long-ranged portion. A useful characterization of the long-wavelength electrostatic response of a system is provided by the Gaussian smoothed charge density

$$\rho^{q\sigma}(\mathbf{r}) \equiv \frac{1}{\sigma^3\pi^{3/2}}\int d\mathbf{r}'\rho^q(\mathbf{r}')e^{-(|\mathbf{r}-\mathbf{r}'|/\sigma)^2} \tag{21}$$

which arises naturally in the context of the local molecular field theory of electrostatic systems.[43,44] The smoothing length σ should be chosen at least on the order of a characteristic nearest neighbor distance, and here we take a conservative choice of $\sigma = 4.5$ Å for smoothing over hydrogen bonds in water. The long-wavelength response from this additional Gaussian smoothing as characterized by $\rho^{q\sigma}(r)$ is in near perfect agreement with the theory, Figure 1B. The accuracy of our approach illustrates that the long-wavelength components of electrostatic behavior follow dielectric continuum theory, even on molecular length scales.

The computed $\breve{G}^l$ for the SPC/E model, shown in Figure 2A for several values of l, indicates that the free energies qualitatively

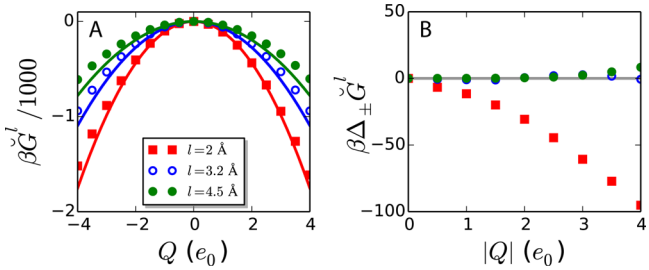

Figure 2. (A) Free energy of inserting a Gaussian test charge into SPC/E water as a function of the charge Q for various values of the width, l. Points correspond to simulation results. Solid lines are the predictions of eq 19. (B) The difference in the insertion free energies $\Delta\breve{G}^l(Q)$ for Gaussian charges of equal magnitude but opposite sign, representing the asymmetry in the insertion free energy with respect to the sign of Q. For l comparable to or greater than the size of a water molecule (i.e., the minimum smoothing length in LMF theory), $\Delta_\pm\breve{G}^l(Q) \approx 0$, such that the response to the Gaussian charge is symmetric and follows linear response theory. Linear response theory breaks down as the width of the Gaussian is reduced.

DOI: 10.1021/acs.jpcb.6b02238
J. Phys. Chem. B 2016, 120, 6238−6249

follow the theory for large l, although finite size corrections are needed for quantitative accuracy.[25,45] At small l, the free energies become asymmetric with respect to Q, disagreeing with the theory. To examine these asymmetries in the free energy with respect to the sign of Q, in Figure 2B we show

$$\Delta_{\pm}\breve{G}^{l}(Q) \equiv \breve{G}^{l}(Q) - \breve{G}^{l}(-Q) \tag{22}$$

the difference in the free energy for the same magnitude of Q but opposite sign.

For large l, $\Delta_{\pm}\breve{G}^{l}$ is symmetric with respect to Q and follows the predictions of eq 19 to a good approximation, evidenced by $\Delta_{\pm}\breve{G}^{l} \approx 0$ in these cases. As l is decreased to 2 Å, the free energies show signs of asymmetry with respect to Q, in qualitative disagreement with the prediction of eq 19. This may be expected because the Gaussian charge density becomes a point charge in the limit $l \to 0$, and the response correspondingly becomes nonlinear and asymmetric with respect to Q.

Although we focus on Gaussian charge distributions, the analogues of eqs 18 and 19 will provide an accurate linear response description for any solute charge density placed in a uniform solvent as long as it is sufficiently weak and slowly varying. Similarly, the formalism is not limited to high dielectric solvents like water.[46] Additionally, we have found that higher order terms in the expansion of the charge−charge linear response function are needed to accurately describe conductors and electrolytes, as described in the Appendix.

Finally, we note that both the structural and thermodynamic responses of many different water models to Gaussian charges will be similar for large l. This is because the response in this limit depends only on ϵ, and many models have similar dielectric constants. Important differences between models emerge when the response becomes nonlinear from strong short-ranged forces, as found when comparing TIP5P and SPC/E water near the cores of hydrophobic solutes.[21] This suggests it could be conceptually and practically useful to rearrange the usual ion solvation process to first focus on a large and essentially universal Gaussian charge component well-described by DCT and then consider the relatively smaller model-dependent nonlinear corrections associated with a detailed description of strong solvent−ion core interactions, as discussed in the next section.

6. THERMODYNAMIC CYCLES ISOLATING NONLINEAR AND ASYMMETRIC CORRECTIONS TO THE BORN MODEL

Here we show that charge-symmetric Born-like contributions to the total charging free energy dominate ion solvation thermodynamics. The remaining portions of the solvation free energy can be nonlinear and asymmetric with respect to Q. Although these terms make up a relatively small percentage of the total (large) ion solvation free energy, their magnitude relative to k_BT can be very significant, and they are qualitatively important for understanding the underlying physics of ion hydration.

By writing the solvation of an ion as a thermodynamic cycle involving an initial insertion of a Gaussian test charge with appropriately chosen width, we first determine a dominant Born-like term. We then can systematically examine the remaining steps, which effectively generate all corrections to dielectric continuum theory.

This new thermodynamic cycle is rooted in concepts underlying the local molecular field (LMF) theory of nonuniform fluids.[43] It allows us to disentangle the effects of core solvation, strong short-ranged ion−solvent interactions, and long-ranged electrostatic interactions on the ion solvation free energy. To develop this cycle, we split the ion−water Coulomb interactions, and consequently the charging process, into short- and long-ranged components. This is accomplished by writing $1/r = v_0(r) + v_1(r)$, where

$$v_0(r) = \frac{\mathrm{erfc}(r/l)}{r} \tag{23}$$

is the short-ranged portion of the potential, and

$$v_1(r) = \frac{\mathrm{erf}(r/l)}{r} \tag{24}$$

is the long-ranged component, equivalent to the electrostatic potential arising from a unit Gaussian test charge distribution of width l. Analogously, $v_0(r)$ is the potential arising from a unit point charge surrounding by a neutralizing Gaussian charge distribution, and thus is short-ranged.

Using this separation of the Coulomb potential, we can rearrange the ion solvation process such that insertion of a Gaussian test charge is the first step in the thermodynamic cycle, as illustrated by Cycle A of Figure 3A. Then, the ionic core is

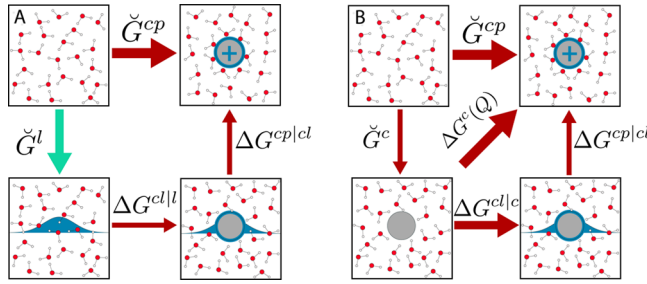

Figure 3. LMF-based thermodynamic cycles for ion solvation: (A) Cycle A and (B) Cycle B. Red arrows indicate steps that contain nonlinear and charge asymmetric terms, while a green arrow indicates that the step follows dielectric continuum theory. The size of the arrows, though not to scale, is meant to give a rough indication of the relative contribution of the step to the total ion solvation free energy. Blue outlines around a core indicate that it contains a charge density (Gaussian or point charge) within it that can be smeared over its surface using Gauss' law.

solvated at the location of the Gaussian charge distribution. In the final step, the short-ranged portion of the ion−solvent electrostatic interaction is turned on, or equivalently, the width of the Gaussian charge distribution is systematically reduced until a delta function point charge is obtained. We will show that broken charge symmetries involved in the last two steps manifest the asymmetric and nonlinear nature of ion solvation.

Table 1 highlights that the first, Born-like step in Cycle A dominates the thermodynamics of ion solvation. There, we list the free energy for each leg of the cycle, and compare the relative importance of the linear and charge-symmetric free energy, $\breve{G}^{l}$, to

Table 1. Free Energies in Cycle A for $Q = \pm 1$ and $l = 3.2$ Å[a]

Q (e_0)	$\beta\breve{G}^{l}$	$\beta\Delta G^{cll}$	$\beta\Delta G^{cp|cl}$	$\beta(\Delta G^{cll} + \Delta G^{cp|cl})$	$\beta\breve{G}^{cp}$
+1	−59 (155)	+31	−10	+21 (−55)	−38
−1	−58 (74)	+15	−35	−20 (26)	−78

[a]In units of k_BT, for a core with a hard sphere radius of 4 Å. Numbers in parentheses indicate relative percentage of $\breve{G}^{cp}$. ΔG^{cll} was obtained using the relation $\Delta G^{cll} = \breve{G}^{cp} - \breve{G}^{l} - \Delta G^{cp|cl}$, where $\breve{G}^{cp}$ was obtained from Cycle B.

DOI: 10.1021/acs.jpcb.6b02238
J. Phys. Chem. B 2016, 120, 6238−6249

the nonlinear and asymmetric portions, $\Delta G^{cll\!l} + \Delta G^{cp\!lcl}$. Note that we have approximated $\Delta G^{cll\!l}(Q)$ by its value at $Q = 0$ in order to get a rough estimate of these relative contributions; $\Delta G^{cll\!l}$ for nonzero Q will only tend to amplify the asymmetries and further support our conclusions.

The data in Table 1 shows that the nonlinear and asymmetric terms comprise 20% of the total solvation free energy (by magnitude), while the first Born-like term of inserting a Gaussian test charge dominates. Thus, we anticipate that thermodynamic cycles like Cycle A will find use in computing solvation free energies of charged solutes. In particular, the majority of the free energy can be determined analytically in the first step with the dielectric continuum theory presented above, while the remaining smaller components of the free energy can be determined through other means.

Moreover, previous work has shown that it may be statistically advantageous to turn on repulsive LJ cores and attractive interactions in concert, but point charge-based electrostatics cannot be turned on until after a repulsive core is inserted.[47] The use of a Gaussian test charge allows for the modification of such frameworks such that the long-ranged part of the electrostatics could be turned on along with or even before the LJ core and attractions, potentially improving statistics of the free energy calculation.

We additionally consider a second cycle, shown in Figure 3B and termed Cycle B, where we first insert an uncharged core into the solvent and then turn on the charge. This makes direct connections with our earlier discussion of the charging free energy and with classic approaches to ion solvation. However, in separate charging steps of the cycle we first turn on the long-ranged portion of the ion−solvent electrostatic interactions, followed by turning on the short-ranged component of the charge. We will show that Cycle B provides additional insight into the role of the electrostatic potential induced by the uncharged core in the first step. In particular, by first turning on only the slowly varying, long-ranged electrostatic interactions, we avoid any strong nonlinear response induced by the strong short-ranged components of the solvent−ion Coulomb interactions. This is accounted for in the last step in the cycle, which is the same for both cycles.

7. CYCLE A: ISOLATING NONLINEAR AND ASYMMETRIC RESPONSE

7.1. Corrections to Born Theory from Insertion of an Uncharged Core. Having already established that the first step of Cycle A, insertion of a Gaussian test charge, follows dielectric continuum theory, we now consider the second step of inserting a solute core in the presence of a Gaussian test charge with width $l = 4.5$ Å. The initial response of SPC/E water to the Gaussian charge density alone is symmetric with respect to the sign of Q and follows linear response theory. However, the insertion of an uncharged core serves to break local charge symmetry in its vicinity,[21] and the free energy associated with this process is asymmetric with respect to the sign of the charge. Moreover, solvation of such excluded volumes is known to be nonlinear, except for very small solutes.

Thus, studying this insertion process in the presence of a Gaussian test charge serves to illustrate that the charge symmetry of the system is not broken prior to core insertion and core insertion breaks this symmetry. We again note that asymmetries arising from this process are at least an order of magnitude smaller than the symmetric Born-like component of the free energy for most ionic solutes. However, these terms may become comparable for large colloidal solutes.

For simplicity, we estimate the free energy of inserting a small solute core, corresponding to a hard sphere with a radius of 2.75 Å. For such small volumes, the free energy can be estimated from equilibrium simulations by monitoring water density fluctuations in a volume v of the same size and shape of the solute.[48] To be specific, the free energy of inserting a hard solute core in the presence of the Gaussian charge is given by

$$\beta \Delta G^{cll\!l} = -\ln P_v(N = 0) \tag{25}$$

where $P_v(N)$ is the probability of observing N water molecules in the volume v, such that $P_v(0)$ is the probability of observing v empty. For larger volumes, umbrella sampling is needed to compute $P_v(N)$.[49] The conditional notation $cll\!l$ used in eq 25 indicates that the transition is from a state with a Gaussian charge distribution with width l to a state cl with the Gaussian embedded in the core.

The water number distributions $P_v(N)$ are shown in Figure 4 for $Q = 0, \pm 1.5$. Density fluctuations in small spherical volumes,

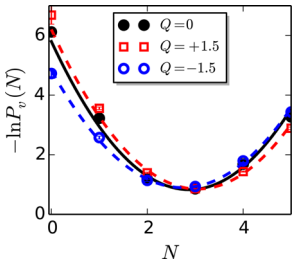

Figure 4. Distribution of the number of water molecules N in a spherical volume with a radius of 2.75 Å located at the center of a Gaussian charge distribution with $l = 4.5$ Å for several values of Q. Here, the negative logarithm of the distribution is shown; this corresponds to the free energy as a function of N such that the free energy of inserting the solute core is equivalent to $\beta \Delta G^{cll\!l} = -\ln P_v(0)$. Lines correspond to Gaussian statistics, and error bars indicate one standard error.

like the one used here, typically follow Gaussian statistics to a good approximation, allowing the insertion free energy to be estimated from the mean and variance of $P_v(N)$ alone. Therefore, we also show the Gaussian estimates of $P_v(N)$ as lines in Figure 4, where the Gaussian estimate is given by

$$-\ln P_v^{\text{Gauss}}(N) = \frac{1}{2}\ln[2\pi\langle(\delta N)^2\rangle_Q] - \frac{(N - \langle N\rangle_Q)^2}{2\langle(\delta N)^2\rangle_Q} \tag{26}$$

$\langle(\delta N)\rangle^2 = \langle N^2\rangle - \langle N\rangle^2$ is the variance of the Gaussian distribution, and $\langle\cdots\rangle_Q$ indicates an ensemble average in the presence of a Gaussian charge distribution with magnitude Q (and width $l = 4.5$ Å).

We find that water density fluctuations are asymmetric with respect to Q, particularly at low N, indicating that the local charge symmetry of the system is broken when the system fluctuates away from $\langle N\rangle_Q$, enabling insertion of a solute core. The fluctuations are Gaussian to a good approximation for small Q, but deviations begin to emerge at large Q, especially for $Q > 0$. The non-Gaussian nature of the density fluctuations indicates that the insertion of a solute core in the presence of a Gaussian charge is nonlinear, even for the small volume considered here, and therefore may not be captured by Gaussian theories.

The asymmetry of the density fluctuations with respect to solute charge manifest in $\Delta G^{cll\!l}$, shown in Figure 5A, which decreases with increasingly negative Q and increases for increasingly

DOI: 10.1021/acs.jpcb.6b02238
J. Phys. Chem. B 2016, 120, 6238−6249

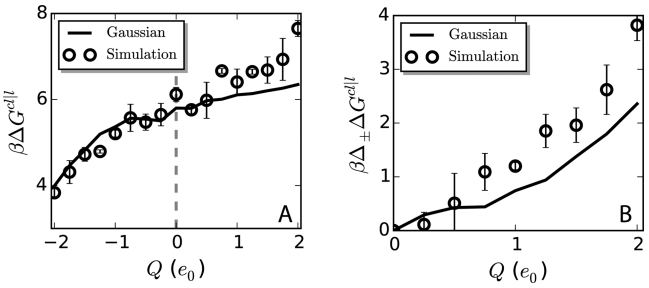

Figure 5. (A) Free energy of inserting a hard sphere with a radius of 2.75 Å located at the center of a Gaussian charge distribution with $l = 4.5$ Å as a function of Q. A distinct asymmetry with respect to the sign of Q is observed. (B) A good measure of this asymmetry is the difference between hard sphere insertion free energies obtained in the presence of Gaussian charges of equal magnitude but opposite sign, $\beta\Delta_{\pm}\Delta G^{cll}(Q)$. Lines are predictions made by assuming Gaussian density fluctuations while data points are obtained from simulation. Error bars indicate one standard error.

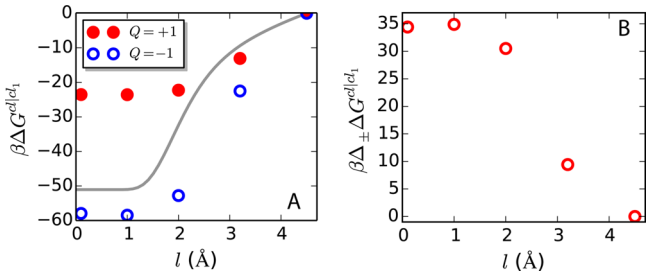

Figure 6. (A) Free energy of shrinking a Gaussian charge density, ΔG^{cllcl_1} with $|Q| = 1$ from $l_1 = 4.5$ Å to $l_2 = 0.1$ Å. The solid line is the prediction of eq 32, which is independent of the sign of the charge. This estimate uses $R = 3$ Å, because this radius refers to the volume from which solvent charge density is excluded. (B) The difference in the shrinking free energies $\Delta_{\pm}\Delta G^{cllcl_1}$ for Gaussian charges of equal magnitude but opposite sign, representing the asymmetry in the free energy with respect to the sign of Q.

positive Q. While this qualitative trend is true even if insertion is symmetric with respect to Q, the difference between hard sphere insertion free energies obtained in the presence of Gaussian charges of equal magnitude but opposite sign, $\Delta_{\pm}\Delta G^{cll}$, clearly illustrates this asymmetry, which is of the same order of magnitude of the core insertion free energy itself (Figure 5B). Moreover, deviations from Gaussian fluctuations of the density are clearly observed by comparing the simulation results (points) with the estimates provided by assuming Gaussian fluctuations (lines) in Figure 5.

We expect all the qualitative findings regarding asymmetry with respect to Q and nonlinearities to be amplified when dealing with larger solute cores. In that case, the distribution $P_v(N)$ even in the absence of charge has large non-Gaussian tails at low N, illustrating that insertion of large cores is highly nonlinear (non-Gaussian) even in the absence of charge, and will remain so if a Gaussian charge is present. Moreover, because the Gaussian charge couples largely to the low N components of $P_v(N)$, one can expect that these tails will respond sensitively to Q (and possibly l).

The nonlinear response to core insertion in the presence of even slowly varying electrostatic fields may have broad implications in the development of general theoretical descriptions of solvation. When an electrostatic potential exists in a fluid prior to core insertion, we find that the response is nonlinear, in contrast to the analogous process for the long-ranged portion of the LJ potential.[50] While this construction may seem artificial, it is precisely what occurs when describing solvation near charged and polar surfaces, like proteins for example. Thus, Gaussian theories of even small solute solvation may break down near molecules or surfaces that exert electric fields on nearby solvent molecules, and one should exercise caution when using such approaches under these conditions.

7.2. Shrinking the Charge Increases Asymmetric Response. We now consider the final step of cycle A, shrinking the Gaussian charge density to a point charge. To compute the free energy of this process, $\Delta G^{cp|cl}$, we perform a set of simulations with a Gaussian charge centered inside a repulsive sphere of radius 4 Å. The width of the Gaussian charge is then varied from $l_1 = 4.5$ Å to $l_2 = 0.1$ Å, at which point the free energy stops changing, because nearly all of the charge is inside the core, effectively creating a point charge inside the core.

The free energy ΔG^{cllcl_1} and its difference with respect to the same magnitude of charge, $\Delta_{\pm}\Delta G^{cllcl_1}$, are shown in Figure 6 for $|Q| = 0.5$ and demonstrate two important points. First, the free energy of shrinking the Gaussian charge is asymmetric, evidenced by the fact that $\Delta G^{cllcl_1}(Q) \neq \Delta G^{cllcl_1}(-Q)$. Second, the process of shrinking the Gaussian charge is nonlinear, as suggested by the form of the simulated free energies.

Despite these differences, the qualitative form and magnitude of the free energy change is closely approximated by DCT (eq 32, described in the next section). Thus, we conjecture that it may be possible to quantitatively describe $\Delta G^{cp|cl}$ using DCT as a reference around which perturbations can be made, accounting for microscopic asymmetries. However, this is beyond the scope of the current work, and we reserve these developments for future investigations.

8. CYCLE B: CHARGING CORES USING GAUSSIANS

We also consider the thermodynamic Cycle B, shown in Figure 3B, in which the solute core is first inserted, and then a Gaussian charge is turned on at the center of the core. This Gaussian is again reduced to a point charge in a final step that is the same as the last step in Cycle A. The first step of this process, inserting an uncharged solute core, has been heavily studied, and we do not re-examine this process here.

Instead, we focus only on the second step of Cycle B, turning on a Gaussian charge distribution at the center of an uncharged solute core. The uncharged solute core breaks the local charge symmetry around the solute and induces a nonzero water charge density.[21] This nonzero charge density makes any subsequent charging step asymmetric with respect to the sign of the charge. We illustrate this here by turning on a Gaussian charge density at the center of a solute hard core or cavity of radius R; this is a charge-symmetric and linear process when carried out in the absence of the core.

In order to obtain a DCT expression for the desired free energy change ΔG^{cllc} we use the same local linear screening picture described in section 3. Again we smear the part of the Gaussian charge density inside the solute core onto its surface using Gauss' law, while leaving the tails of the Gaussian outside that already overlap the solvent unchanged. The total charge inside the core is given by

$$Q_{\text{in}} = 4\pi \int_0^R \mathrm{d}r r^2 Q\rho_{\text{G}}(r) \tag{27}$$

$$= \frac{Q}{l\sqrt{\pi}}\left[l\sqrt{\pi}\,\text{erf}\left(\frac{R}{l}\right) - 2Re^{-R^2/l^2}\right] \tag{28}$$

DOI: 10.1021/acs.jpcb.6b02238
J. Phys. Chem. B 2016, 120, 6238−6249

Thus, the equivalent overlapping solute charge density is

$$\rho^{Q}(r) \approx \begin{cases} -Q_{\text{in}}\dfrac{\delta(r-R)}{4\pi r^2} + Q\rho_{\text{G}}(r) & r \geq R \\ 0 & r < R \end{cases} \tag{29}$$

and the solvent response is assumed to be

$$\rho^{q}(r) \approx \begin{cases} -\left(1-\dfrac{1}{\epsilon}\right)\rho^{Q}(r) & r \geq R \\ 0 & r < R \end{cases} \tag{30}$$

The expression for the free energy

$$\Delta G^{cl|c} = \int_0^1 \mathrm{d}\lambda\lambda \int \mathrm{d}\mathbf{r}\rho^{q}(\mathbf{r})v_{Q}(r) \tag{31}$$

can then be readily integrated to obtain the DCT approximation

$$\Delta G^{cl|c} = -\frac{Q_{\text{in}}^2}{2R}\left(1-\frac{1}{\epsilon}\right) - \frac{Q^2}{l\sqrt{2\pi}}\left(1-\frac{1}{\epsilon}\right) \times \left[\operatorname{erfc}\left(\frac{R\sqrt{2}}{l}\right) + \sqrt{2}\operatorname{erf}\left(\frac{R}{l}\right)e^{-R^2/l^2}\right] \tag{32}$$

This free energy smoothly interpolates between the respective Gaussian test charge and Born theory limits: $\lim_{R\to 0}\Delta G^{cl|c} = \breve{G}^{l}$ and $\lim_{l\to 0}\Delta G^{cl|c} = \Delta G^{cp|c} = \Delta G^{c}(Q)$.

We show in the Supporting Information that these same results can be obtained from a Gaussian field model[51] derived in the spirit of dielectric continuum theory. We find that focusing initially on the charge density rather than the free energy functional simplifies the theoretical framework and clarifies the physical assumptions made in DCTs.

The free energy $\Delta G^{cl|c}$ obtained from simulation for $R = 4$ Å is shown in Figure 7A and is asymmetric with respect to the sign of Q, even for large l. This is better illustrated by considering the difference in insertion free energies for the same magnitude of Q but opposite sign, $\Delta_{\pm}\Delta G^{cl|c}$, Figure 7B. Even for the largest width studied, significant asymmetries are observed for for high $|Q|$ (although they are at least an order of magnitude smaller than the total charging free energy).

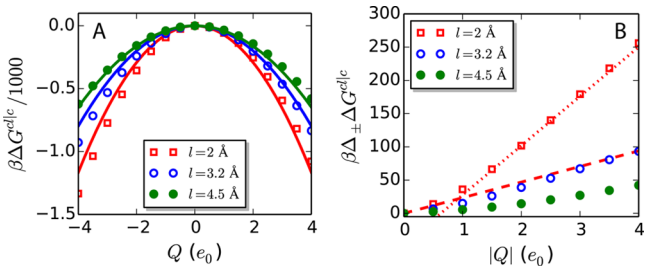

Figure 7. (A) Free energy $\Delta G^{cl|c}$ of inserting a Gaussian charge density into a hard solute core of radius 4 Å for three values of l. In all cases, the charging free energy is asymmetric about $Q = 0$ due to the nonzero charge density around the core even in the absence of charge. Solid lines represent the predictions of eq 32 with $R = 3$ Å, because the volume in the theory should exclude all charge. (B) The difference between the insertion free energies for charges of equal magnitude but opposite sign, $\Delta_{\pm}\Delta G^{cl|c}$, which quantifies the asymmetry in the insertion free energy with respect to the sign of Q. Clearly, $\Delta G^{cl|c}$ is highly asymmetric with respect to the sign of Q, with it being more favorable to insert a negatively charged Gaussian distribution. The dashed line is the prediction from eq 33, while the dotted line is that from eq 34 for $Q_0 = 2$, both for the case of $l = 2$ Å.

Equation 32 lacks the asymmetry contained in the simulation results, but provides a good estimate of the order of magnitude of the charging free energy, in complete analogy to the description of point charge ion solvation provided by Born theory. This suggests that the response to the Gaussian charge is linear beyond the charge asymmetry; this is elaborated upon in the next section. Indeed, successful extensions to the Born model have been developed that account for charge asymmetry through the introduction of fitting parameters without a qualitative change in the linear response form of the free energy.[8,9]

Finally, we note that if eq 20 is used to relate the Gaussian width l to the Born radius R_{B}, then the Born-like models derived above predict that $\Delta G^{l}(Q) \equiv \breve{G}^{l} = \Delta G^{c}(Q)$ or effectively that the (charge asymmetric) diagonal red arrow in Figure 3B can be replaced by the (charge-symmetric) green arrow in Figure 3A. This further use of the Born approximation thus predicts, for example, that $\breve{G}^{l} = \Delta G^{cl|c} + \Delta G^{cp|cl}$. However, the only step in any of the cycles that satisfies the Born approximation quantitatively is that for $\breve{G}^{l}$, the insertion of a Gaussian test charge with large width l, as labeled by the green arrow in Figure 3A. As shown above, even the final step in both cycles is not quantitatively described by a Born-like theory.

Thus, in general $\breve{G}^{l} \neq \Delta G^{cl|c} + \Delta G^{cp|cl}$ as a direct consequence of the nonlinearities and asymmetries that contribute to the free energies on the right-hand side, evidenced by the data in Tables 1 and 2. Similar ideas underly the breakdown of other relations that can be derived from this use of the Born approximation in Figure 3B. For example, Born theory would also lead to $\breve{G}^{l}$ being equal to $\breve{G}^{cp} - \breve{G}^{c}$, but the data in Tables 1 and 2 also indicate that this equality does not hold, again demonstrating the quantitative inaccuracy of this Born-like theory.

Table 2. Free Energies in Cycle B for $Q = \pm 1$ and $l = 3.2$ Å[a]

$Q\ (e_0)$	$\beta\breve{G}^{c}$	$\beta\Delta G^{cl|c}$	$\beta\Delta G^{cp|cl}$	$\beta\breve{G}^{cp}$
+1	+20	−48	−10	−38
−1	+20	−63	−35	−78

[a]In units of $k_{\text{B}}T$, for a core with a hard sphere radius of 4 Å. The DCT estimate for $\breve{G}^{cp}$ does not include a contribution from $\breve{G}^{c}$.

8.1. Linear Response Regimes of Gaussian Core Charging in Water. Interestingly, the free energy difference $\Delta_{\pm}\Delta G^{cl|c}$ appears to have two linear regimes for all l-values for SPC/E water; we have also observed an analogous existence of two linear regimes in TIP5P water, although the asymmetry is much smaller in that case. The first regime roughly corresponds to $Q \leq 1$, but will in general depend on l and R. This linear regime is highlighted by the dashed line in the bottom panel of Figure 7B. A transition from one linear regime to another then occurs, after which $\Delta_{\pm}\Delta G^{cl|c}$ scales linearly with Q, but with a different slope than in the first regime, as indicated by the dotted line in Figure 7B.

These two regimes can be understood from the structural response of water to the Gaussian-charged core. At $Q = 0$, the hydrogen bond network of SPC/E water is maintained around the solute, but water molecules still tend to orient their dipoles toward the solute, resulting in a net negative electrostatic potential in the solute core with respect to that in the bulk solvent. Correspondingly, hydrogen density is high slightly inside the core boundary, resulting in a positive peak in the charge density $\rho^{q}(r)$, as shown in Figure 8A. When inserting a Gaussian

DOI: 10.1021/acs.jpcb.6b02238
J. Phys. Chem. B 2016, 120, 6238−6249

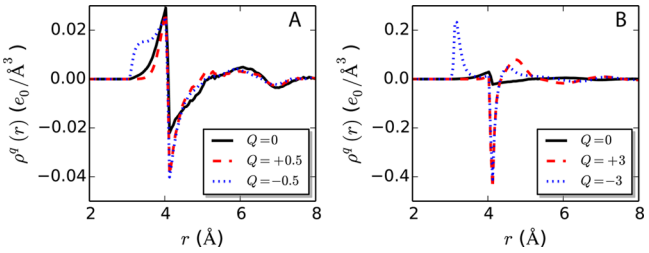

Figure 8. (A) Charge density $\rho^q(r)$ as a function of distance from the solute core for charges in the first linear response regime. The structure is only slightly perturbed about the $Q = 0$ case when $Q < 1$. (B) Charge densities in the second linear response regime differ dramatically from the $Q = 0$ case. However, further increasing Q in the positive or negative direction does not change the qualitative features of the charge density, such that increases in Q result in a linear response about the respective (sign-dependent) reference systems.

charge distribution with a small Q (or large l), the water structure around the core is not significantly perturbed, and the solvent responds linearly about the $Q = 0$ system. Therefore, $\Delta_{\pm}\Delta G^{cllc}$ can be approximated by

$$\Delta_{\pm}\Delta G^{cllc}(Q) = 2|Q|\langle V_l\rangle_0 \tag{33}$$

where $V_1 \equiv V_1(\overline{\mathbf{R}}) = \sum_{i=1}^{N_C} q_i v_l(\mathbf{r}_i(\overline{\mathbf{R}}))$ is the total interaction energy between the N_C charged solvent sites in the system and the Gaussian charge distribution, divided by the charge of the Gaussian. Indeed, the linear response theory estimate provided by eq 33 yields an accurate description of $\Delta_{\pm}\Delta G^{cllc}$ in this first regime, as shown by the dashed line in Figure 7B.

As the magnitude of the charge becomes large $(1-2e_0)$, the water structure around the core begins to change substantially. Large reorientations begin to point hydrogen atoms directly into the solute core when $Q < 0$, and comparably large reorientations direct O−H bonds away from the solute when $Q > 0$. Correspondingly, a large positive peak well within the hard solute core develops in $\rho^q(r)$ when $Q < -2$, and all positive charge density inside the core vanishes when $Q > +2$, Figure 8B. The transition region $1 \leq Q \leq 2$ arises from these structural changes.

Beyond $Q = 2$, the structural response of water to the Gaussian charge does not qualitatively change; i.e., there are no significant reorientations of water molecules that change the general features of $\rho^q(r)$. Therefore, the solvent again responds linearly, but about these new solvation structures ($|Q| \approx 2$), which differ for positive and negative charges. When the reference state is taken to be $Q_0 \neq 0$, we can again use linear response theory to approximate the free energy difference

$$\Delta_{\pm}\Delta G^{cllc}(Q) = \Delta_{\pm}\Delta G^{cllc}(Q_0) + |Q - Q_0|[\langle V_1\rangle_{Q_0} - \langle V_1\rangle_{-Q_0}] \tag{34}$$

where we now have a different reference state for positive and negative charges (here taken to be of the same magnitude Q_0), and we have assumed that fluctuations in the energy about the two reference states are the same, which is a good approximation. The linear response theory approximation given by eq 34 indeed provides a good estimate of $\Delta_{\pm}\Delta G^{cllc}$ in this second linear regime, as indicated by the dashed line in Figure 7B obtained for $Q_0 = 2$.

The presence of two linear response regimes may have significant implications for understanding specific ion effects. In particular, many interesting phenomena are observed for multivalent ions that are absent in their monovalent counterparts.[1,5,52] These unique effects may be related to multivalent ions being in the high Q LRT regime, which results from very strong, nonlinear distortions of the hydration shell with respect to the $Q \leq 1$ states.

We note that although the transition region and the location of the two linear regimes are similar for all l values shown here, one would anticipate that the boundaries between these regimes will depend on the solute size and shape. Additionally, the relative sensitivity of these regimes to l should also depend on the nature of the solute (i.e., size and shape). However, a thorough investigation of the l and R-dependence is beyond the scope of the current work.

9. SIMULATION DETAILS

Molecular dynamics (MD) simulations were performed using the DL_POLY version 2.18 software package,[53] modified to include the Gaussian charge and excluded volume potentials used throughout this work. Ion cores are described using the hyperbolic tangent potential employed in previous work.[21] All simulations were performed in the isothermal−isobaric (constant NPT) ensemble using a Berendsen thermostat and barostat[54] to maintain the temperature and pressure of the system at T = 300 K and P = 1 atm. Electrostatic interactions between water molecules were evaluated using Ewald summation,[30] with a real space cutoff of 9 Å and a precision of 10^{-6}. Solute−solvent electrostatic interactions were computed using direct summation to ensure that the solvent response follows the expected asymptotics for an infinite system and is not distorted by Ewald summation techniques.[55] This approach leads to small artifacts localized near the edge of the box, and any molecules within 10 Å from the box edge were neglected when computing properties.

APPENDIX: DERIVATION AND ANALYSIS OF GAUSSIAN TEST CHARGE INSERTION IN ELECTROLYTES

As a more stringent test of our ideas, we apply the above dielectric continuum formalism to a conductor, the symmetric primitive model (SPM) electrolyte, the response of which will be trivially symmetric with respect to the sign of the Gaussian charge distribution. Instead of the traditional SPM, which consists of charged hard spheres of equal diameter, whose hard core potential is difficult to treat using standard MD packages, we use harshly repulsive but continuous charged Weeks−Chandler−Andersen (WCA) spheres with equal Lennard-Jones (LJ) diameters.[56]

In a conducting medium, $\epsilon = \infty$, and eq 18 becomes

$$\rho^q(\mathbf{r}) = -\frac{Q}{l^3\pi^{3/2}}e^{-r^2/l^2} \tag{35}$$

By assuming a local linear response, the induced charge density is now equal and opposite to the applied Gaussian charge distribution itself, and the total charge density of the system is zero for all $\mathbf{r}$! While this is consistent with the zeroth moment complete screening condition of Stillinger and Lovett,[38−40,57] this lowest order approximation for the *total charge density* in a conducting fluid has no nonzero terms, and it is clear that additional terms in the small k expansion of the charge density are needed for an accurate description of the response of a conducting fluid to a Gaussian test charge.

We follow the treatment developed in eq 16 for describing Gaussian charge solvation but keep terms to fourth order in k in the expansion of the charge−charge linear response function

$$\hat{\chi}_0^{qq}(\mathbf{k}) \sim k^2\hat{\chi}_0^{(2)qq} + k^4\hat{\chi}_0^{(4)qq} \tag{36}$$

DOI: 10.1021/acs.jpcb.6b02238
J. Phys. Chem. B 2016, 120, 6238−6249

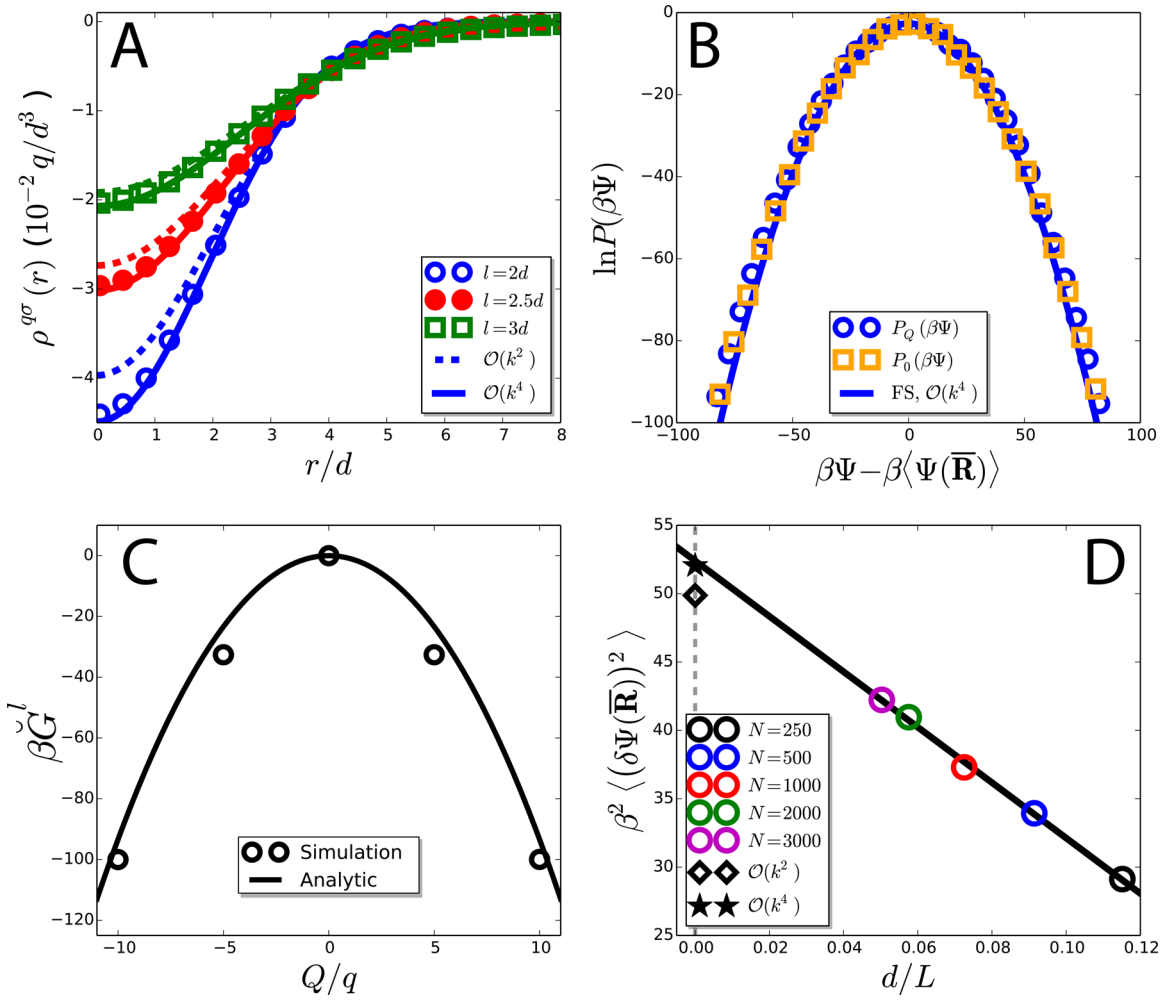

Figure 9. (A) Gaussian smoothed charge densities of the SPM in response to Gaussian charge distributions of varying width with $Q = 5q$. Symbols are simulation results; the approximations to second and fourth order in the expansion of the linear response function are indicated by dashed lines and solid lines, respectively. Gaussian smoothing was performed using $\sigma = 2d$. (B) Probability distributions of the interaction energy Ψ for a Gaussian test charge of magnitude $Q = 5d$ and $l = 2d$. The solid line is the corresponding analytic approximation. (C) Free energy of inserting a Gaussian test charge with width $l = 2d$ as a function of Q/q. (D) Variance of the interaction energy as a function of L^{-1} for a Gaussian test charge with $Q = 5d$ and $l = 2d$. The solid line is a linear fit to the data points, and the starred data point is given by eq 40.

to obtain

$$\rho^q(\mathbf{r}) = -\frac{Q}{l^3\pi^{3/2}}e^{-r^2/l^2} + \frac{4\pi\beta Q\hat{\chi}_0^{(4)qq}}{l^5\pi^{3/2}}\left[\left(\frac{2r}{l}\right)^2 e^{-r^2/l^2} - 6e^{-r^2/l^2}\right] \tag{37}$$

for the charge density response induced by the Gaussian charge distribution and

$$\breve{G}^l = -\frac{Q^2}{l\sqrt{2\pi}}\left(1 + \frac{4\pi\beta\hat{\chi}_0^{(4)qq}}{l^2}\right) \tag{38}$$

for the free energy change upon insertion of the test charge density.

The generalized Debye−Hückel (GDH) theory of Lee and Fisher[58−60] provides an expression for the fourth-moment of the charge−charge linear response function

$$\hat{\chi}_{0,\mathrm{GDH}}^{(4)qq} = \rho\xi_D^4\left[1 + \frac{2}{3}\ln(1+x) - \frac{2}{3}x - \frac{1}{6}x^2\right] \tag{39}$$

where $\xi_D = \sqrt{k_BT/(8\pi q^2\rho)}$ is the Debye length, q is the magnitude of the charge of the ions, ρ is the ensemble-averaged number density of the electrolyte in the volume V, and $x = d/\xi_D$ is the diameter of an ion in units of the Debye length. The GDH theory satisfies both the zeroth and second moment conditions of Stillinger and Lovett,[38−40,58,60] and yields exact results for correlations in the low density limit. However, GDH predictions are only semiquantitative, and in general will not yield accurate estimates of $\hat{\chi}_0^{(4)qq}$ for all ρ and Γ. Nevertheless, simulation results[60] seem to indicate that, at our chosen state point, which is far from the critical point, GDH theory will yield reasonable estimates for the fourth moment of the linear response function, and indeed we find this to be true.

We probe the response of a neutral SPM composed of $N = N_+ + N_- = 1000$ ions at a density of $\rho d^3 = 0.3816$ and a coupling strength of $\Gamma = \beta q^2/d = 5$ to Gaussian test charges of varying width and magnitude, where $d \approx \sigma_{LJ}$ is the approximate diameter of an ion of the SPM, with an LJ well depth of $\varepsilon_{LJ} = k_BT$. For all Q and l studied, we find that terms of order k^4 in the expansion of the linear response function (which are of order k^2 in the small-k expansion of the nonuniform charge density $\rho^q(\mathbf{r})$)

DOI: 10.1021/acs.jpcb.6b02238
J. Phys. Chem. B 2016, 120, 6238−6249

are needed to accurately describe the structural response for all r, as exemplified by the Gaussian smoothed charge densities shown in Figure 9. However, as expected, at large enough r both expressions for the induced charge density converge to the same value and accurately describe the asymptotic charge density response.

Fluctuations in the test charge-SPM interaction energy follow Gaussian statistics for all systems under study in agreement with the continuum theory, as evidenced by the distributions in Figure 9B. In addition, simulation results obtained by varying N from 250 to 3000 ions yield the L^{-1} scaling behavior expected from theory, and the $L \to \infty$ limit obtained from extrapolation agrees well with the continuum theory estimate

$$\langle (\delta\Psi(\bar{R}))^2 \rangle = \frac{2k_BTQ^2}{l\sqrt{2\pi}}\left(1 + \frac{4\pi\beta\hat{\chi}_0^{(4)qq}}{l^2}\right) \tag{40}$$

as shown in Figure 9D. In contrast, neglect of terms of order k^4 in the expansion of the charge−charge linear response function leads to an underestimation of the infinite system limit as obtained from simulation, illustrated by the point labeled $O(k^2)$ in Figure 9D. The free energies of inserting a Gaussian test charge as a function of Q/q in Figure 9C are also in good agreement with the theory developed here.

■ ASSOCIATED CONTENT

Supporting Information

The Supporting Information is available free of charge on the ACS Publications website at DOI: 10.1021/acs.jpcb.6b02238.

Charge density-based Gaussian field theory model of solvation in a dielectric and additional discussion of ion solvation thermodynamics in the context of dielectric continuum theory (PDF)

■ AUTHOR INFORMATION

Corresponding Authors

*E-mail: rremsing@temple.edu.

*E-mail: jdw@umd.edu.

Notes

The authors declare no competing financial interest.

■ ACKNOWLEDGMENTS

We acknowledge funding from NSF CHE-1300993. We also acknowledge insightful discussions with David Chandler, Marcel Baer, Greg Schenter, Chris Mundy, Ang Gao, Patrick Shaffer, and Stephen Cox.

■ REFERENCES

(1) Collins, K. D. Why Continuum Electrostatics Theories Cannot Explain Biological Structure, Polyelectrolytes or Ionic Strength Effects in Ion-Protein Interactions. *Biophys. Chem.* **2012**, *167*, 43−59.

(2) Ball, P. Water as an Active Constituent in Cell Biology. *Chem. Rev.* **2008**, *108*, 74−108.

(3) Tobias, D. J.; Stern, A. C.; Baer, M. D.; Levin, Y.; Mundy, C. J. Simulation and Theory of Ions at Atmospherically Relevant Aqueous Liquid-Air Interfaces. *Annu. Rev. Phys. Chem.* **2013**, *64*, 339−59.

(4) Levin, Y.; dos Santos, A. P. Ions at Hydrophobic Interfaces. *J. Phys.: Condens. Matter* **2014**, *26*, 203101.

(5) Collins, K. D. Charge Density-Dependent Strength of Hydration and Biological Structure. *Biophys. J.* **1997**, *72*, 65−76.

(6) Born, M. Volumes and Hydration Warmth of Ions. *Eur. Phys. J. A* **1920**, *1*, 45−48.

(7) Hünenberger, P.; Reif, M. *Single Ion Solvation. Experimental and Theoretical Approaches to Elusive Thermodynamic Quantities*; The Royal Society of Chemistry: Cambridge, U.K., 2011.

(8) Rajamani, S.; Ghosh, T.; Garde, S. Size Dependent Ion Hydration, its Asymmetry, and Convergence to Macroscopic Behavior. *J. Chem. Phys.* **2004**, *120*, 4457.

(9) Bardhan, J. P.; Jungwirth, P.; Makowski, L. Affine-Response Model of Molecular Solvation of Ions: Accurate Predictions of Asymmetric Charging Free Energies. *J. Chem. Phys.* **2012**, *137*, 124101.

(10) Ashbaugh, H. S. Convergence of Molecular and Macroscopic Continuum Descriptions of Ion Hydration. *J. Phys. Chem. B* **2000**, *104*, 7235−7238.

(11) Harder, E.; Roux, B. On the Origin of the Electrostatic Potential Difference at a Liquid-Vacuum Interface. *J. Chem. Phys.* **2008**, *129*, 234706.

(12) Beck, T. L. The Influence of Water Interfacial Potentials on Ion Hydration in Bulk Water and Near Interfaces. *Chem. Phys. Lett.* **2013**, *561*−*562*, 1−13.

(13) Shi, Y.; Beck, T. L. Length Scales and Interfacial Potentials in Ion Hydration. *J. Chem. Phys.* **2013**, *139*, 044504.

(14) Wilson, M. A.; Pohorille, A.; Pratt, L. R. Comment on "Study on the Liquid-Vapor Interface of Water. I. Simulation Results of Thermodynamics Properties and Orientational Structure. *J. Chem. Phys.* **1989**, *90*, 5211−5213.

(15) Pratt, L. R. Contact Potentials of Solution Interfaces: Phase Equilibrium and Interfacial Electric Fields. *J. Phys. Chem.* **1992**, *96*, 25−33.

(16) Leung, K.; Rempe, S. B.; von Lilienfeld, O. A. Ab Initio Molecular Dynamics Calculations of Ion Hydration Free Energies. *J. Chem. Phys.* **2009**, *130*, 204507.

(17) Leung, K.; Marsman, M. Energies of Ions in Water and Nanopores within Density Functional Theory. *J. Chem. Phys.* **2007**, *127*, 154722.

(18) Kathmann, S. M.; Kuo, I.-F. W.; Mundy, C. J.; Schenter, G. K. Understanding the Surface Potential of Water. *J. Phys. Chem. B* **2011**, *115*, 4369−4377.

(19) Baer, M. D.; Stern, A. C.; Levin, Y.; Tobias, D. J.; Mundy, C. J. Electrochemical Surface Potential Due to Classical Point Charge Models Drives Anion Adsorption to the Air-Water Interface. *J. Phys. Chem. Lett.* **2012**, *3*, 1565−1570.

(20) Horváth, L.; Beu, T.; Manghi, M.; Palmeri, J. The Vapor-Liquid Interface Potential of (Multi)polar Fluids and its Influence on Ion Solvation. *J. Chem. Phys.* **2013**, *138*, 154702.

(21) Remsing, R. C.; Baer, M. D.; Schenter, G. K.; Mundy, C. J.; Weeks, J. D. The Role of Broken Symmetry in Solvation of a Spherical Cavity in Classical and Quantum Water Models. *J. Phys. Chem. Lett.* **2014**, *5*, 2767−2774.

(22) Asthagiri, D.; Pratt, L. R.; Ashbaugh, H. S. Absolute Hydration Free Energies of Ions, Ion-Water Clusters, and Quasichemical Theory. *J. Chem. Phys.* **2003**, *119*, 2702−2708.

(23) Vorobjev, Y. N.; Hermans, J. A Critical Analysis of Methods of Calculation of a Potential in Simulated Polar Liquids: Strong Arguments in Favor of "Molecule-Based" Summation and of Vacuum Boundary Conditions in Ewald Summation. *J. Phys. Chem. B* **1999**, *103*, 10234−10242.

(24) Kastenholz, M. A.; Hünenberger, P. H. Computation of Methodology-Independent Ionic Solvation Free Energies from Molecular Simulations. I. The Electrostatic Potential in Molecular Liquids. *J. Chem. Phys.* **2006**, *124*, 124106.

(25) Hummer, G.; Pratt, L. R.; García, A. E. Free Energy of Ionic Hydration. *J. Phys. Chem.* **1996**, *100*, 1206−1215.

(26) Duignan, T. T.; Parsons, D. F.; Ninham, B. W. A Continuum Model of Solvation Energies Including Electrostatic, Dispersion, and Cavity Contributions. *J. Phys. Chem. B* **2013**, *117*, 9421−9429.

(27) Hummer, G.; Pratt, L. R.; García, A. E. Multistate Gaussian Model for Electrostatic Solvation Free Energies. *J. Am. Chem. Soc.* **1997**, *119*, 8523−8527.

(28) Hyun, J.-K.; Ichiye, T. Nonlinear Response in Ionic Solvation: A Theoretical Investigation. *J. Chem. Phys.* **1998**, *109*, 1074−1083.

DOI: 10.1021/acs.jpcb.6b02238
J. Phys. Chem. B 2016, 120, 6238−6249

(29) Zangwill, A. *Modern Electrodynamics*; Cambridge University Press, 2013.
(30) Allen, M. P.; Tildesley, D. J. *Computer Simulation of Liquids*; Oxford: New York, 1987.
(31) Chialvo, A. A.; Cummings, P. T. Simple Transferable Intermolecular Potential for the Molecular Simulation of Water Over Wide Ranges of State Conditions. *Fluid Phase Equilib.* **1998**, *150−151*, 73−81.
(32) Sprik, M.; Klein, M. L. A Polarizable Model for Water Using Distributed Charge Sites. *J. Chem. Phys.* **1988**, *89*, 7556−7560.
(33) Kiss, P. T.; Baranyai, A. A Systematic Development of a Polarizable Potential of Water. *J. Chem. Phys.* **2013**, *138*, 204507−18.
(34) Coslovich, D.; Hansen, J.-P.; Kahl, G. Ultrasoft Primitive Model of Polyionic Solutions: Structure, Aggregation, and Dynamics. *J. Chem. Phys.* **2011**, *134*, 244514.
(35) Warren, P. B.; Masters, A. J. Phase Behaviour and the Random Phase Approximation for Ultrasoft Restricted Primitive Models. *J. Chem. Phys.* **2013**, *138*, 074901.
(36) Chandler, D. The Dielectric Constant and Related Equilibrium Properties of Molecular Fluids: Interaction Site Cluster Theory Analysis. *J. Chem. Phys.* **1977**, *67*, 1113−1124.
(37) Rodgers, J. M.; Weeks, J. D. Accurate Thermodynamics for Short-Ranged Truncations of Coulomb Interactions in Site-Site Molecular Models. *J. Chem. Phys.* **2009**, *131*, 244108.
(38) Stillinger, F. H.; Lovett, R. General Restriction on the Distribution of Ions in Electrolytes. *J. Chem. Phys.* **1968**, *49*, 1991−1994.
(39) Stillinger, F. H.; Lovett, R. Ion-Pair Theory of Concentrated Electrolytes. I. Basic Concepts. *J. Chem. Phys.* **1968**, *48*, 3858−3868.
(40) Lovett, R.; Stillinger, F. H. Ion-Pair Theory of Concentrated Electrolytes. II. Approximate Dielectric Response Calculation. *J. Chem. Phys.* **1968**, *48*, 3869−3884.
(41) Martin, P. A. Sum Rules in Charged Fluids. *Rev. Mod. Phys.* **1988**, *60*, 1075−1127.
(42) Remsing, R. C.; Liu, S.; Weeks, J. D. Long-Ranged Contributions to Solvation Free Energies from Theory and Short-Ranged Models. *Proc. Natl. Acad. Sci. U. S. A.* **2016**, *113*, 2819−2826.
(43) Rodgers, J. M.; Weeks, J. D. Local Molecular Field Theory for the Treatment of Electrostatics. *J. Phys.: Condens. Matter* **2008**, *20*, 494206.
(44) Remsing, R. C.; Weeks, J. D. Hydrophobicity Scaling of Aqueous Interfaces by an Electrostatic Mapping. *J. Phys. Chem. B* **2015**, *119*, 9268−9277.
(45) Hummer, G.; Pratt, L. R.; García, A. E. Molecular Theories and Simulation of Ions and Polar Molecules in Water. *J. Phys. Chem. A* **1998**, *102*, 7885−7895.
(46) Remsing, R. C. *From Structure to Thermodynamics with Local Molecular Field Theory*. Ph.D. Thesis, University of Maryland, 2013.
(47) Naden, L. N.; Shirts, M. R. Linear Basis Function Approach to Efficient Alchemical Free Energy Calculations. 2. Inserting and Deleting Particles with Coulombic Interactions. *J. Chem. Theory Comput.* **2015**, *11*, 2536−2549.
(48) Hummer, G.; Garde, S.; García, A. E.; Pohorille, A.; Pratt, L. R. An Information Theory Model of Hydrophobic Interactions. *Proc. Natl. Acad. Sci. U. S. A.* **1996**, *93*, 8951−8955.
(49) Patel, A. J.; Varilly, P.; Chandler, D.; Garde, S. Quantifying Density Fluctuations in Volumes of All Shapes and Sizes using Indirect Umbrella Sampling. *J. Stat. Phys.* **2011**, *145*, 265−275.
(50) Remsing, R. C.; Patel, A. J. Water Density Fluctuations Relevant to Hydrophobic Hydration are Unaltered by Attractions. *J. Chem. Phys.* **2015**, *142*, 024502.
(51) Chandler, D. Gaussian Field Model of Fluids With an Application To Polymeric Fluids. *Phys. Rev. E* **1993**, *48*, 2898−2905.
(52) Beck, T. L. A Local Entropic Signature of Specific Ion Hydration. *J. Phys. Chem. B* **2011**, *115*, 9776−9781.
(53) Smith, W.; Yong, C.; Rodger, P. DL_POLY: Application to Molecular Simulation. *Mol. Simul.* **2002**, *28*, 385−471.
(54) Berendsen, H. J. C.; Postma, J. P. M.; van Gunsteren, W. F.; DiNiola, A.; Haak, J. R. Molecular Dynamics with Coupling to an External Bath. *J. Chem. Phys.* **1984**, *81*, 3684.
(55) Figueirido, F.; Buono, G. S. D.; Levy, R. M. On Finite-Size Effects in Computer Simulations Using the Ewald Potential. *J. Chem. Phys.* **1995**, *103*, 6133−6142.
(56) Denesyuk, N. A.; Weeks, J. D. A New Approach for Efficient Simulation of Coulomb Interactions in Ionic Fluids. *J. Chem. Phys.* **2008**, *128*, 124109.
(57) Hansen, J. P.; McDonald, I. R. *Theory of Simple Liquids*; Elsevier Ltd., 2006.
(58) Lee, B. P.; Fisher, M. E. Density Fluctuations in an Electrolyte from Generalized Debye-Hückel Theory. *Phys. Rev. Lett.* **1996**, *76*, 2906−2909.
(59) Lee, B. P.; Fisher, M. E. Charge Oscillations in Debye-Hückel Theory. *Europhys. Lett.* **1997**, *39*, 611−616.
(60) Das, S. K.; Kim, Y. C.; Fisher, M. E. Near Critical Electrolytes: Are the Charge-Charge Sum Rules Obeyed? *J. Chem. Phys.* **2012**, *137*, 074902.

DOI: 10.1021/acs.jpcb.6b02238
J. Phys. Chem. B 2016, 120, 6238−6249